THE MEASUREMENT, INTERPRETATION AND USE OF UNSTEADY MOMENTUM FLUXES IN TWO-PHASE FLOW

Tien Sieh Yih
Peter Griffith

Report No. 70318-50
Contract No. AT(30-1)-3496

Department of Mechanical Engineering
Engineering Projects Laboratory
Massachusetts Institute of Technology

August 1967

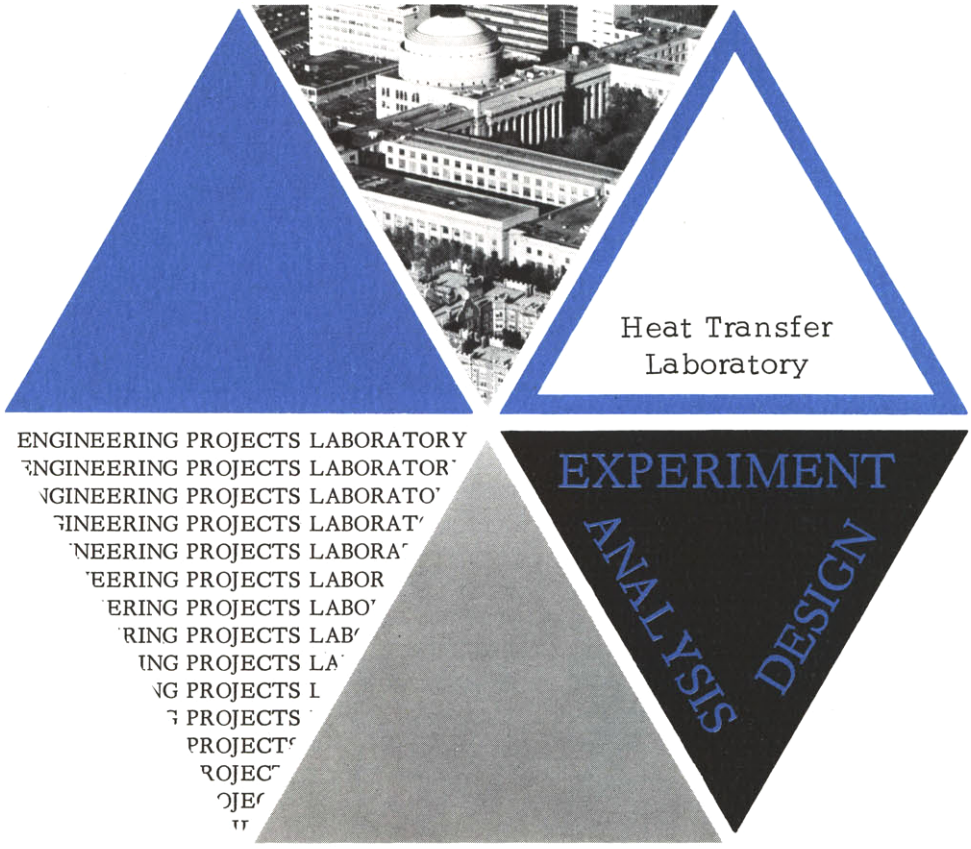

THE MEASUREMENT, INTERPRETATION AND USES OF UNSTEADY MOMENTUM FLUXES IN TWO-PHASE FLOW

Tien Sieh Yih
Peter Griffith

Report No. 70318-50

Contract No. AT(30-1)-3496

August 1967

Department of Mechanical Engineering
Massachusetts Institute of Technology
Cambridge, Massachusetts

ABSTRACT

The steady and unsteady components of the momentum flux in a two-phase flow have been measured at the exit of a vertical pipe by means of an impulse technique using a turning tee and beam. Different electrical filters have been tried in the recording circuit for eliminating the signals around the natural frequency of the beam system. A special filter set has been designed to approximate the inverse of the transfer function of the beam system. Thus the signals recorded after passing through the beam-filter combination can be considered as the excitation times a constant. Two different analog methods have been used to analyze the random signals for obtaining some statistical quantities such as the predominant frequency and the rms value of the unsteady momentum flux. These quanities are useful in some applications involving two-phase flow. In the preliminary measurements of the unsteady momentum flux for the adiabatic up flow of an air-water mixture in a 5/8 inch pipe, the greatest unsteadiness of momentum flux appeared in the quality range of one per cent to six per cent. Above ten per cent quality no appreciable fluctuation has been detected. In an example problem, using the preliminary results, the effect of the unsteady momentum flux on a fuel rod has been studied. The amplitude of the vibrations resulting from the two-phase excitation has been found. In addition it has also been found that there is a possibility of unstable vibrations due to a nonlinear restoring force on the fuel element. This nonlinearity is due to the unsteady component of the momentum flux in the flow past the rod.

TABLE OF CONTENTS

LIST OF FIGURES

1. INTRODUCTION

It is well known that a two-phase flow is basically unsteady in that the pressure, the void fraction, and the momentum flux all vary with time. The complete description of a two-phase flow should include information relating to its unsteady nature. In spite of this, there are only two studies of the unsteady components of a two-phase flow. One is a systematic investigation of the fluctuating pressure of two-phase flow in horizontal pipes with an air-water mixture which was carried out by Semenov[1]+. His method of data reduction was not specified. Therefore, the use of his results is limited. Pressure-time measurements of an air-water system have also been made by Hubbard and Dukler[2]. Random vibration techniques were applied in their data processing. Because they primarily aimed at the characterization of flow regimes, complete data of fluctuating wall pressure was not presented.

Measurements of either one of the three time varying quantities, void fraction, pressure or momentum flux, in a two-phase flow would develop insight into flow mechanics and provide useful information for some applications. However, the momentum flux variations are the most convenient to work with because they are defined experimentally at a surface while the void fraction and pressure drop are defined over a volume and a length, respectively. Furthermore, the information about unsteady momentum fluxes may be helpful in answering some important application questions. For instance, the structural vibrations in reactor fuel elements may be excited by the unsteady component of the momentum flux. To date quite a few papers studying the fluid-induced vibrations of fuel elements have been published[3, 4, 5, 6, 7]. In most of them investigations were restricted to single-phase flow. Only Paidoussis made the attempt to deal with two-phase flow by introducing a time independent void fraction into the density term of his empirical expression. A fluctuating flow can excite vibrations which no steady flow can, and such a model will not show these vibrations.

+Numbers in parentheses are listed in the Bibliography on page 34 .

In the present investigation, the measured unsteady momentum flux data for a two-phase air-water up flow was machine processed using standard random vibration techniques. This data was then fed into a simplified fuel rod model and the vibration amplitude due to the two-phase flow momentum flux fluctuations was established. Different methods for predicting the vibration amplitude of the fuel rod were discussed.

2. DESCRIPTION OF EXPERIMENT

The experimental apparatus is shown schematically in Figs. 1 and 2. This is a modification of Andeen's apparatus which was used in the investigation of steady momentum flux[8]. By means of a turning tee the momentum flux of the two-phase flow at the exit plane of the vertical test pipe is converted into a force which acts upon the beam built inside the pressure vessel. The displacement of the beam is then picked up by the Linear Variable Differential Transformer (LVDT). After being amplified and filtered the signals are recorded on magnetic tape.

2.1 Fluids Feed System

The layout of the feed system of steam, air, and water is shown in Fig. 1. Some changes were made upon the old system.

To utilize the full capacity of the existing equipment the piping connecting two pumps was rearranged so that the main pump and auxiliary pump can work either simultaneously or separately to feed or circulate water. In addition to the original 5.7 gal./min. rotometer a 19.3 gal./min. rotometer was installed into the water supply line. Correspondingly, the size of water outlet line was increased to 2 inches. These changes have significantly increased the water supplying capacity which is needed for tests in the low flow quality region at high flow velocity. The air supply line pressure fluctuation was found to be in the range of 10 per cent of the mean supply pressure. In the measurement of unsteady momentum flux such pressure fluctuations are intolerable. Hence a pressure regulator was used to eliminate this problem.

2.2 Turning Tee and Beam

In the unsteady momentum flux measurement, the turning tee and beam combination is a dynamic system. The momentum flux of two-phase flow is the excitation to this system and the beam displacement is the response. The trend of some earlier investigations[1, 2] into the unsteady nature of two-phase flow shows that the significant fluctuation of two-phase flow are of relatively low frequencies. Therefore, in order to obtain the fluctuating behavior of the excitation from the response it is desirable to have a dynamic system with high natural frequency. By increasing the stiffness and reducing the weight of the system its natural frequency was increased from 44 cycles per second to 84 cycles per second.

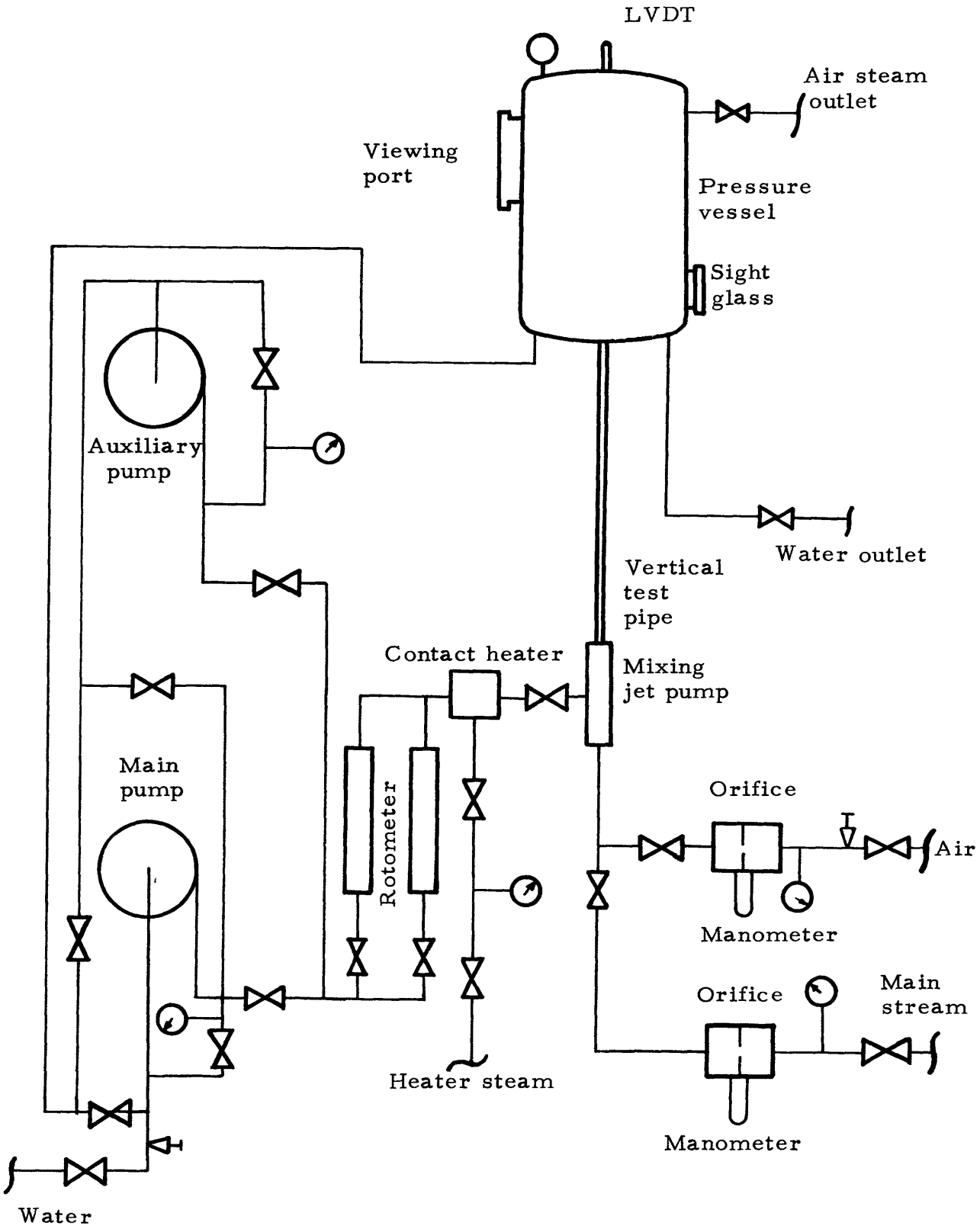

Fig. 1. Arrangement of Apparatus (A).

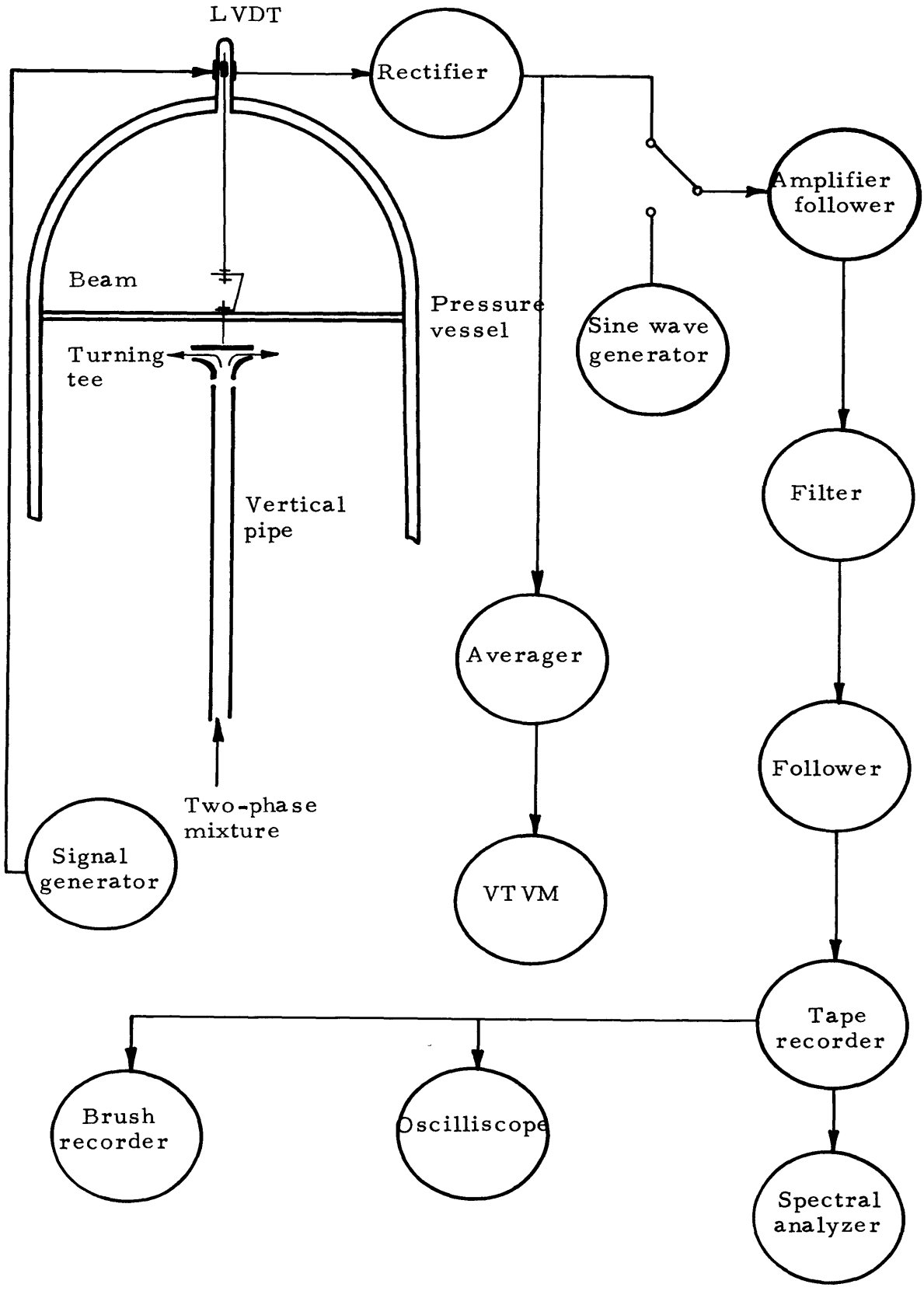

Fig. 2. Arrangement of Apparatus (B).

2.3 Recording Circuit and Filter

As shown in Fig. 2, one output from the rectifier goes to the Vacuum Tube Voltmeter (VTVM) through an averager. The reading on the VTVM is proportional to the time averaging of the momentum flux. Another output goes through the amplifier and the filter and then to the tape recorder. The follower before the tape recorder is an amplifier of unity gain being used to prevent the recorder from drawing too much current out of the circuit. The oscilliscope and brush recorder are connected to the playback of the tape recorder. While signals are being recorded on the tape they can be visualized on the oscilliscope. The input of the amplifier can be switched over to receive signals from the sine wave generator to check the electronic drift in the circuit and for calibration.

The filter is used primarily to attenuate the signals at the natural frequency of the beam system. This can be accomplished by the following different filter systems:

A. A low pass filter is able to serve this purpose. As it is not commercially available, a first order, three-stage low pass filter has been built. The filter circuit and performance are shown in Figs. 3 and 4 respectively. The attenuation at the system natural frequency, i.e., 84 cps, is good. But signals at frequencies other than 84 cps are also affected. This undesirable effect can be compensated for mathematically during the transferring process for the power spectral density curve.

B. An active second order low pass filter can be used to compensate the dynamic effect of the beam system. This filter has the property that its transfer function is approximately the inverse of the beam transfer function at the low frequency range. When this filter is put in series with the beam system, the resulting output, within the low frequency range, is equal to the excitation times a constant. Such a filter is shown in Fig. 5.

C. The filter shown in Fig. 5 can be combined with a ten-stage low pass filter having a sharp cut off before the 84 cps natural frequency of the beam system. This system gives an output signal which is almost unaffected by the dynamic characteristics of the beam system and reflects only the excitation.

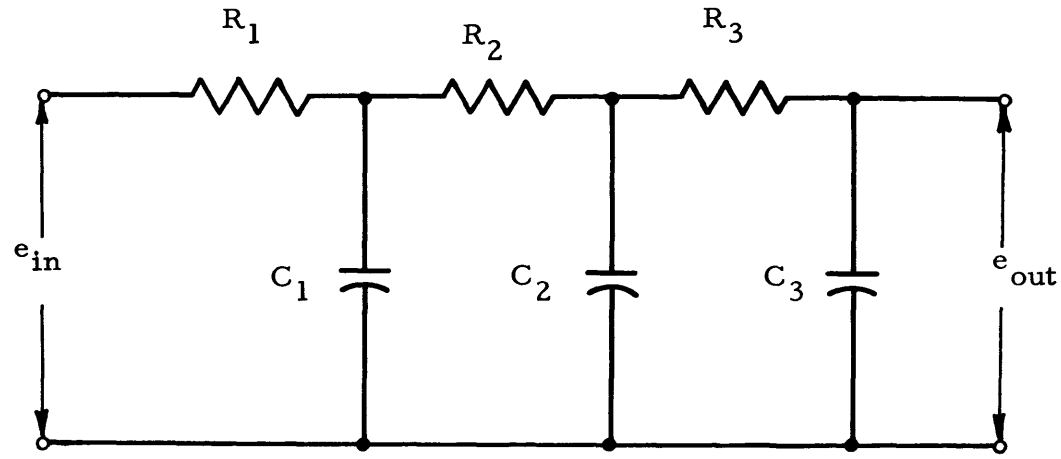

$C_1 = 10\ \mu f$; $C_2 = 1\ \mu f$ $C_3 = 0.1\ \mu f$

$R_1 = 0.82\ k\Omega$ $R_2 = 8.2\ k\Omega$ $R_3 = 82\ k\Omega$

Fig. 3. Circuit Diagram of Filter (A).

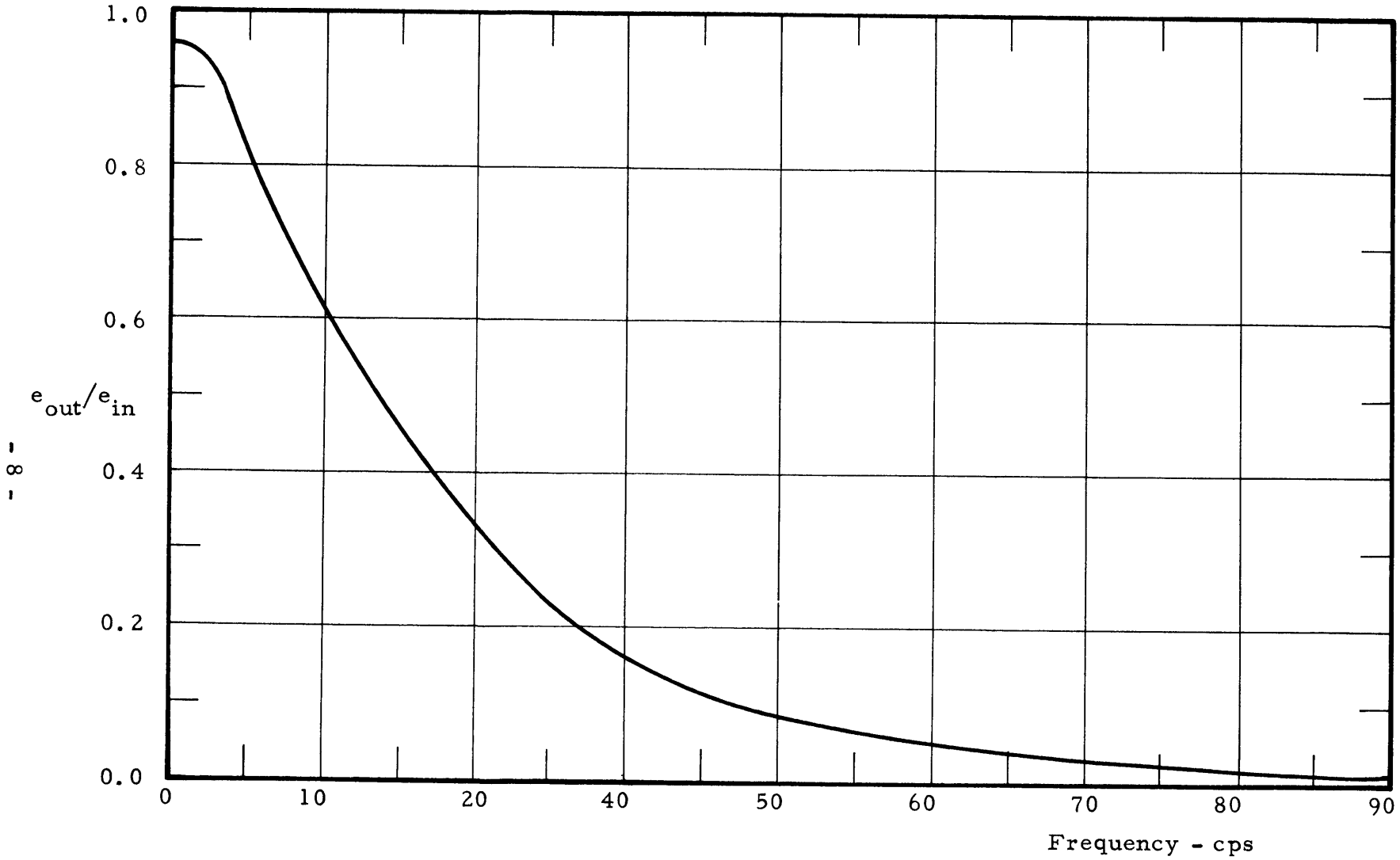

Fig. 4. Performance Curve of Filter (A).

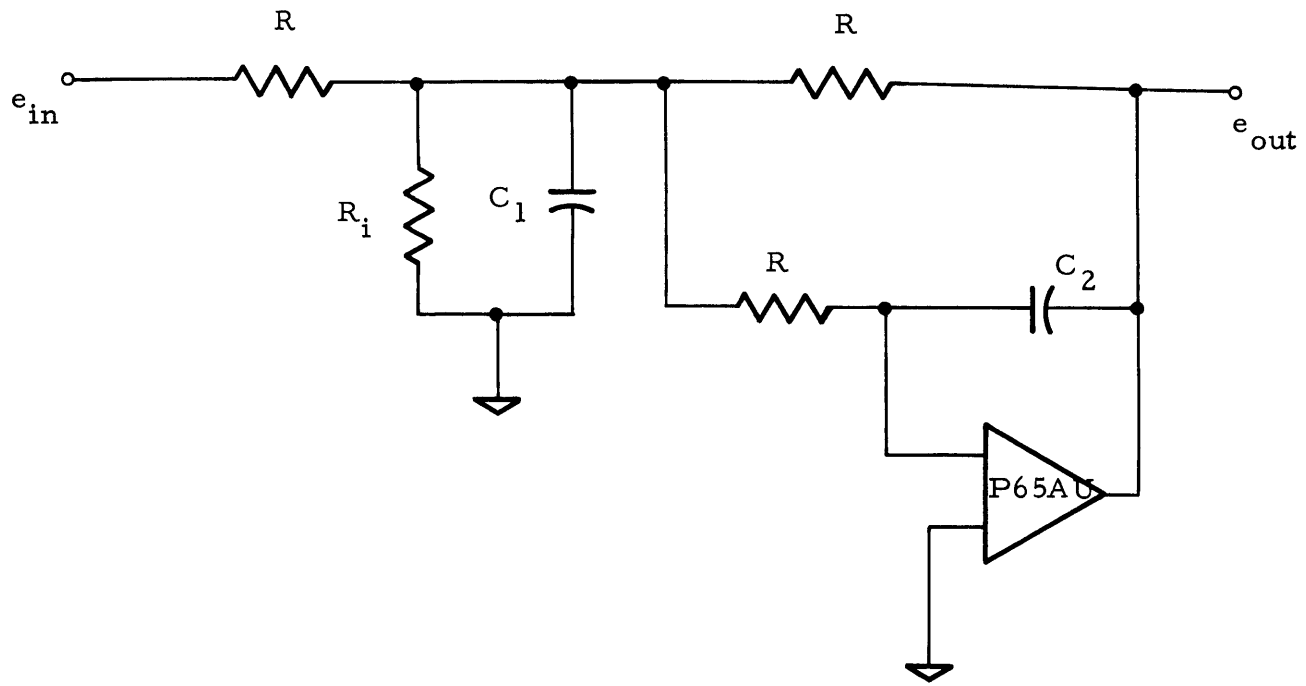

$C_1 = 0.25\ \mu f$ $\qquad$ $C_2 = 0.0025\ \mu f$

$R = 100\ k\Omega$ $\qquad$ $R_i = 7.7\ k\Omega$

Fig. 5. Circuit Diagram of Filter (B).

Filter A is the simplest one to make and was used in the early stage of this investigation. By using this filter in the recording circuit the recorded signal is the distorted response of the beam system. A transferring process is necessary for acquiring the information of the excitation. Using filter system C one can obtain the excitation information without any transferring process. In comparison with system C, filter B is much simplier yet can also give signals reflecting the excitation in the relatively low frequency range. As mentioned before, the significant fluctuations of two-phase flow are of relatively low frequencies. Therefore, this filter system was considered the most suitable for use in this application. However, due to its poor attenuating function at the natural frequency of the beam system, the energy in the recorded signal was mainly that of the beam natural frequency and the portion of energy in the low frequency range was too small to be usable for data processing. To overcome this difficulty a commercial band pass filter was connected in series with filter B, to decrease the energy level at the beam natural frequency. The performance curve of this combined filter system is shown in Fig. 6 where the reciprocal of the beam transfer function is also presented for comparison. Since this combined filter satisfactorily meets the requirements of this experiment, it will be used in the recording circuit for further measurements of the unsteady momentum flux.

2.4 Exploratory Tests

Some preliminary runs have been conducted with a 5/8 inch test pipe at atmospheric pressure and adiabatic flow conditions. Appendix C gives the data obtained from the tests with an air-water mixture. In tests No. 1 through 12, filter A was used in the recording circuit. Whereas, test No. 13 is a typical run using the combined system of filter B and the band pass filter.

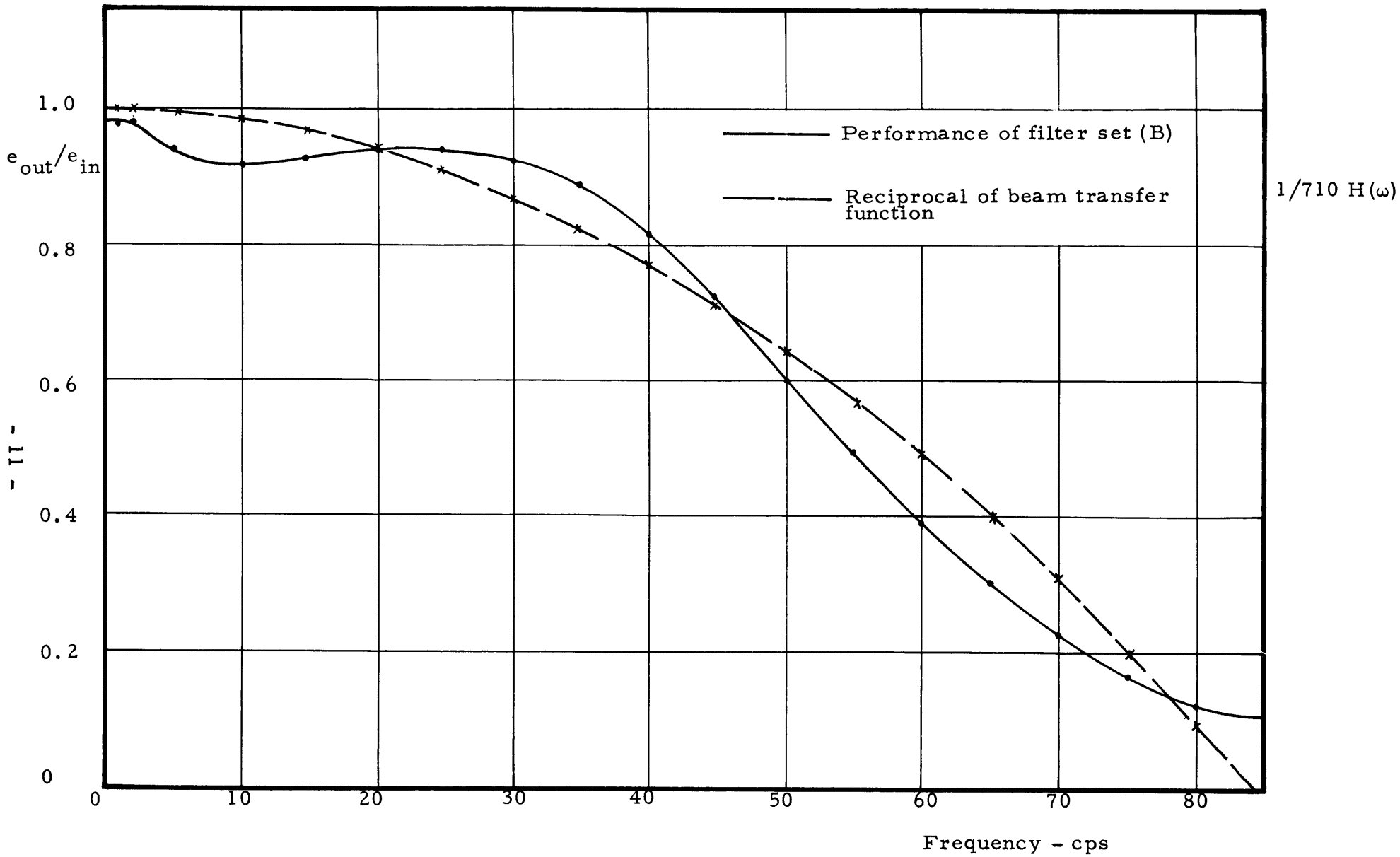

Fig. 6. Performance Curve of Combined Filter Set and Reciprocal of Beam Transfer Function.

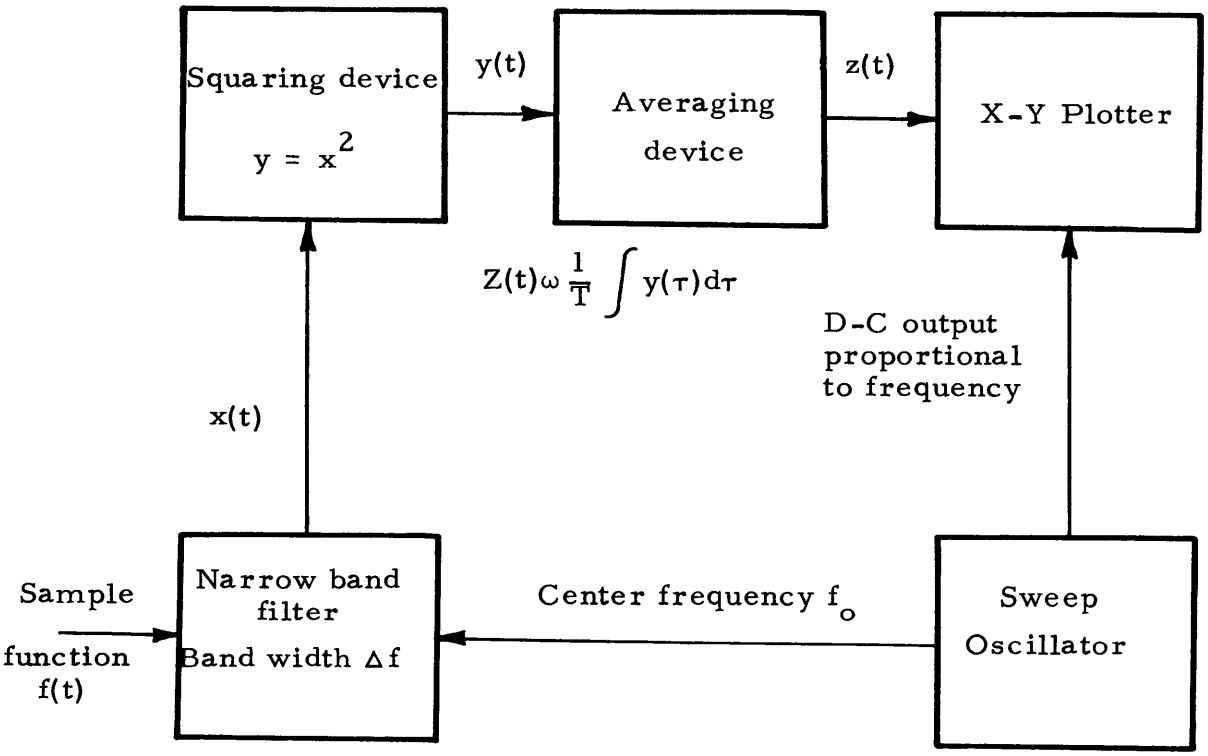

Fig. 7. Spectral Analysis System (linear plot)

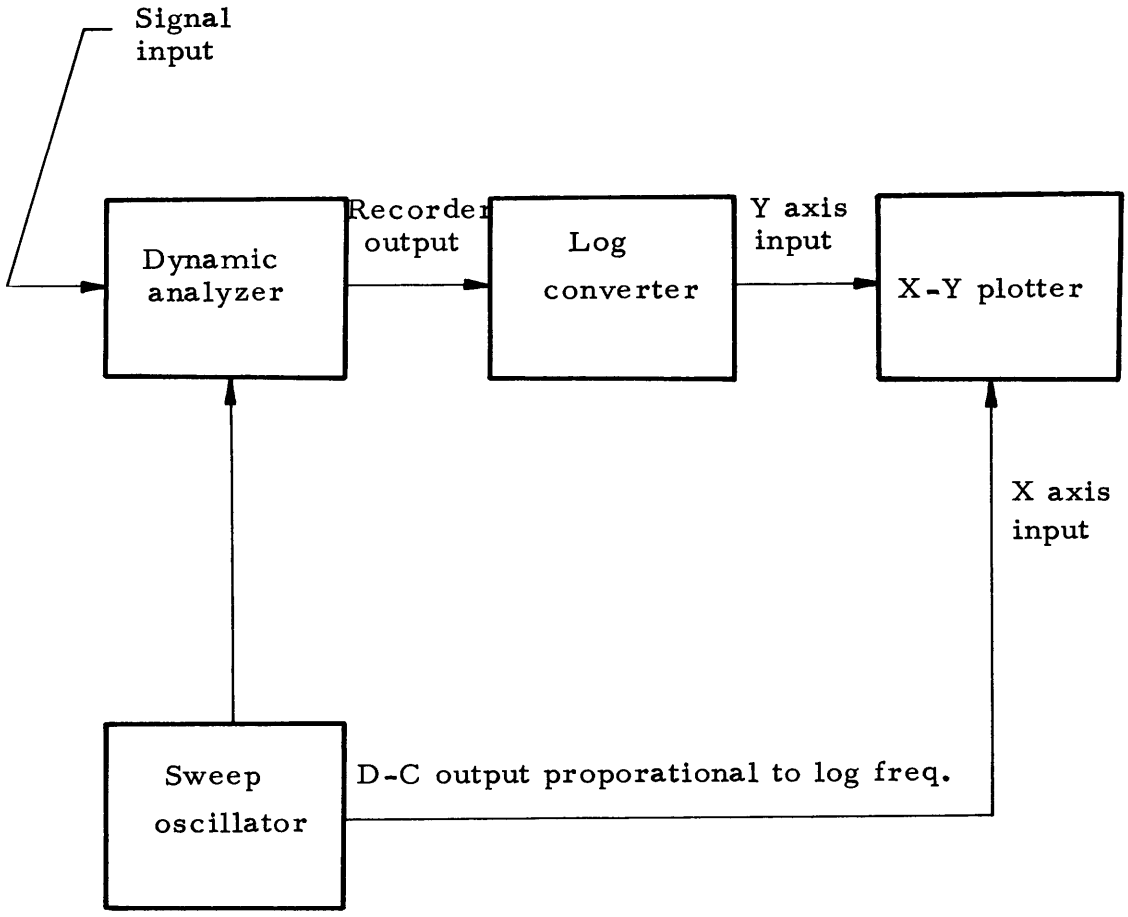

Fig. 8. Spectral Analysis System (db plot)

3. DATA PROCESSING

3.1 Power Spectral Density Curve

By applying the random vibration techniques, the power spectral density curve of the momentum flux of a two-phase flow can be constructed from the signals recorded on the magnetic tape. This process can be carried out by several different methods. They are divided broadly into the digital and the analog methods. In the case of the digital method it is necessary that the recorded signals go through a digitalizing process to convert them into discrete numbers. Then the spectral analysis program can be set up and performed by digital computer[9]. At M.I.T. the analog equipment is available but the complete digitizing facilities are not. The analog equipment is negligible in operation cost in comparison with the digital computer, and is ready for use. Thus only the analog techniques have been applied for spectral analysis.

The procedure commonly used in power spectral density measurement can be represented by the block diagram shown in Fig. 7[10]. The sample function f(t) is the signal played back from tape recorder. The filtering process in the first block is carried out by the SD 101 A Dynamic Analyzer in which there is a narrow band filter with fixed band width $\Delta f = 5$ cps. The SD 104-5 Sweep Oscillator is used to perform an automatic sweep of the center frequency f_o. The analog computer unit K5-M provides the squaring function in the second block. To average the squared signals continuously the following differential equation is applied,

$$\frac{T^2}{12}\ddot{Z} + \frac{T}{2}\dot{Z} + Z = y \qquad (1)$$

where T is the averaging time[11]. Two K5-U computer units are employed as the averaging device to solve Eq. 1. The final output Z(t) is plotted versus the sweeping center frequency f_o on the X-Y plotter. The Z vs. f curve thus obtained is a linear plot from which it is very convenient to find the rms value of momentum flux or to perform some transferring process.

The block diagram shown in Fig. 8 is one of the alternatives for spectral analysis. Being connected with a capacitor set the Dynamic

Analyzer can accomplish both the filtering and averaging processes. The squaring device used in the previous method is replaced by a Log Converter. This method will give the power spectral density curve in a logarithmic plot, which is good for the spectral analysis with wide ranges of frequency and energy level.

3.2 Transfer of the Power Spectral Density Curve

In case filter A is used in the recording circuit the signals recorded on magnetic tape are the distorted time history of beam displacement. Hence the Z vs. f curve obtained from the spectral analysis process is $Z(f) = G_x(f) \cdot (F(f))^2$, where $G_x(f)$ denotes the power spectral density curve of beam displacement and F(f) is the performance curve of filter A, as shown in Fig. 4. The spectral density curve of the unsteady momentum flux is $G_p(f) = G_x(f)/|H(2\pi f)|^2$ with $H(2\pi f) = H(\omega)$ in Eq. 28. Therefore,

$$G_p(f) = \frac{Z(f)}{|H(\omega)|^2 \left[F(f)\right]^2} \qquad (2)$$

The operations indicated in Eq. 2 can be carried out in several different ways:

A. Graphical Method - The Curve $(F(f))^2$ is first constructed from the F(f) curve in Fig. 4. In the frequency range of interest sufficient number of points should be chosen and at each point the value of $|H(\omega)^2|$ computed. The values of Z(f) and $(F(f))^2$ are measured from the diagrams with appropriate scales. Thus the value of $G_p(f)$ at each chosen frequency can be calculated to obtain the power spectral density curve.

B. Analytical Method - The Z(f) curve is approximated by some simple shape curve so that it can be expressed in equation form as a function of frequency f. The filter performance curve F(f) should also be written as an equation in terms of f. Then from Eq. 2, $G_p(f)$ can be represented by an equation in f.

C. Automatic Method - Fig. 9 shows the block diagram of this method. This diagram differs from the one in Fig. 7 by the addition of two blocks i.e., the function forming device and the multiplying device. Once the expression of $\tau(f) = 1/|H(\omega)|^2 (F(f))^2$ in terms of f has been found it is just

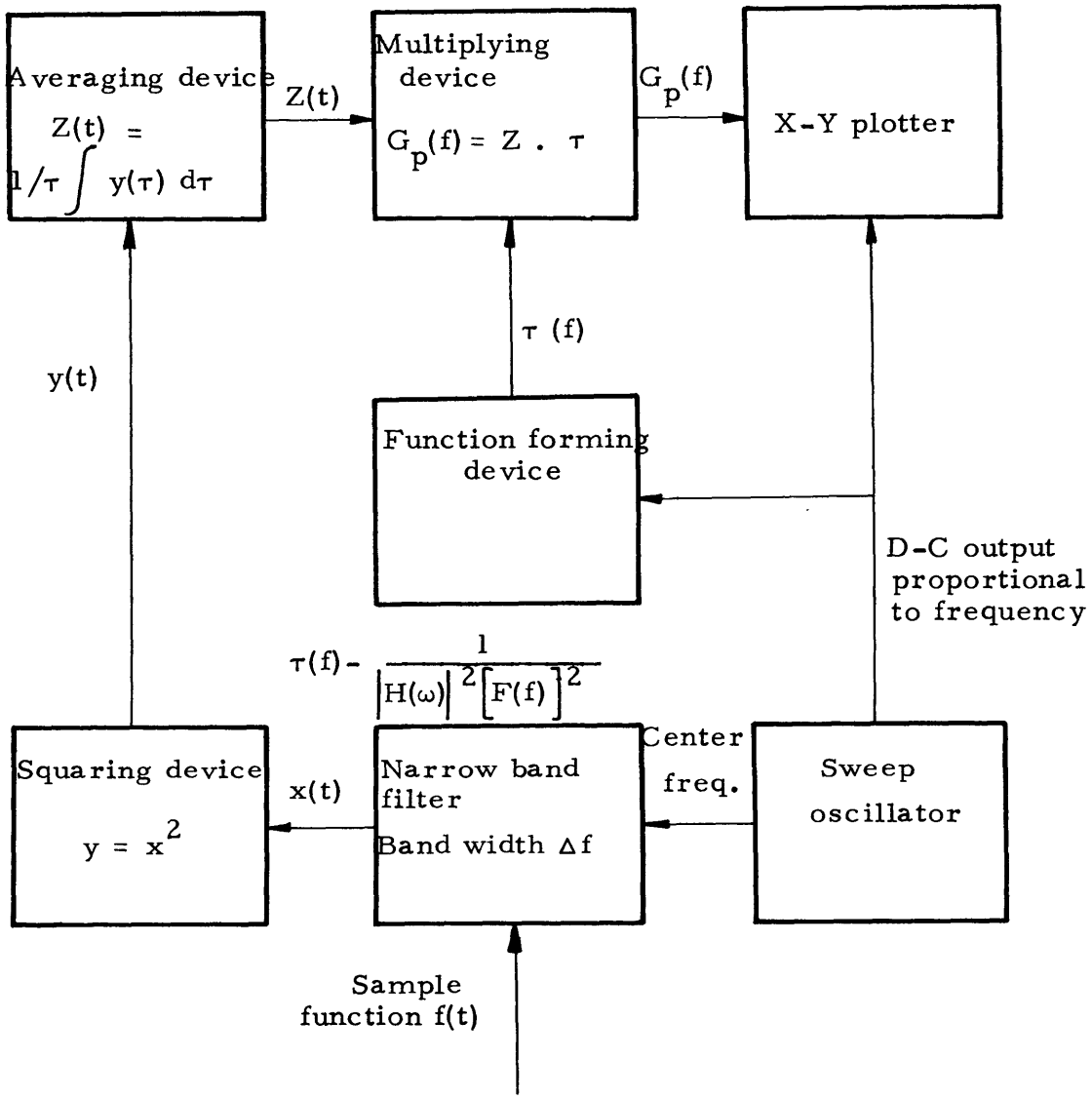

Fig. 9. Spectral Analysis System with Automatic Transferring Device.

a matter of using more computer units such as K5-M and K5-U. With this arrangement the spectral analysis and the transferring process will be completed at the same time.

Among these transferring methods the automatic method is the best one for dealing with a large amount of spectral analysis data, because it can save the manual work required in the other two methods. As the number of spectral density curves being transferred decreases, this advantage will be overshadowed by the extra work in setting up the function forming device in the spectral analysis system. Hence for the transferring of few spectral density curves the graphical method is preferable. The analytical method is good only when it is necessary to express the spectral density curve as a function in terms of frequency.

3.3 Root Mean Square Value

There are commerical instruments which can measure the rms value directly from random signals. Due to the presence of the beam system in the momentum flux measuring process a considerable portion of the energy in the recorded signals is at the natural frequency of the beam system, even after severe attenuation. Thus by direct measurement one would expect to get an rms value of momentum flux much higher than its true value. Under these circumstances, the indirect measurement of rms value must be adopted. In this method, the rms value is obtained by measuring the area under the power spectral density curve $G_p(f)$. Since

$$E(P^2) = \int_0^\infty G_p(f)df \qquad (3)$$

and the rms value is the square root of Eq. 3. From the spectral density curves obtained in the exploratory tests it has been seen that beyond 50 cps the magnitude of unsteady momentum flux in two-phase flow is very small. As an approximation the upper integration limit in Eq. 3 can be replaced by 50. In other words, to calculate the rms value one need only measure the area under the curve up to 50 cps. Thus the trouble due to the beam natural frequency being at 84 cps can be avoided.

4. ANALYTICAL EXAMPLE

4.1 Fuel Rod Model

To show the effect of the unsteady momentum flux on a two-phase flow system a simplified model simulating the fuel rod of a reactor is established. As shown in Fig. 10, this model is a rod simply supported at both ends immersed in a much simplified slug flow which is flowing in the longitudinal direction of the rod.

By defining the void fraction of the two-phase mixture

$$\alpha = \frac{l_g}{l_f + l_g} \tag{4}$$

and the period of the liquid plug

$$T_p = \frac{l_f + l_g}{V} \tag{5}$$

then we have its frequency

$$\omega_k = \frac{2\pi\alpha V}{l_g} \tag{6}$$

Suppose the density of the flow at a section varies sinusoidally. It can be expressed as

$$\rho = \frac{\rho_f}{2}(1 - \alpha)\left[1 + \sin \omega_k (t - \tau)\right] \tag{7}$$

where

$$\tau = \int_{L-y}^{y} \frac{dy}{V} = \frac{y}{V} \tag{8}$$

As an approximation, the transverse force acting on an element length dy of the rod is

$$dF = \frac{\delta}{\frac{L}{2}} \rho V^2 D\, dy \tag{9}$$

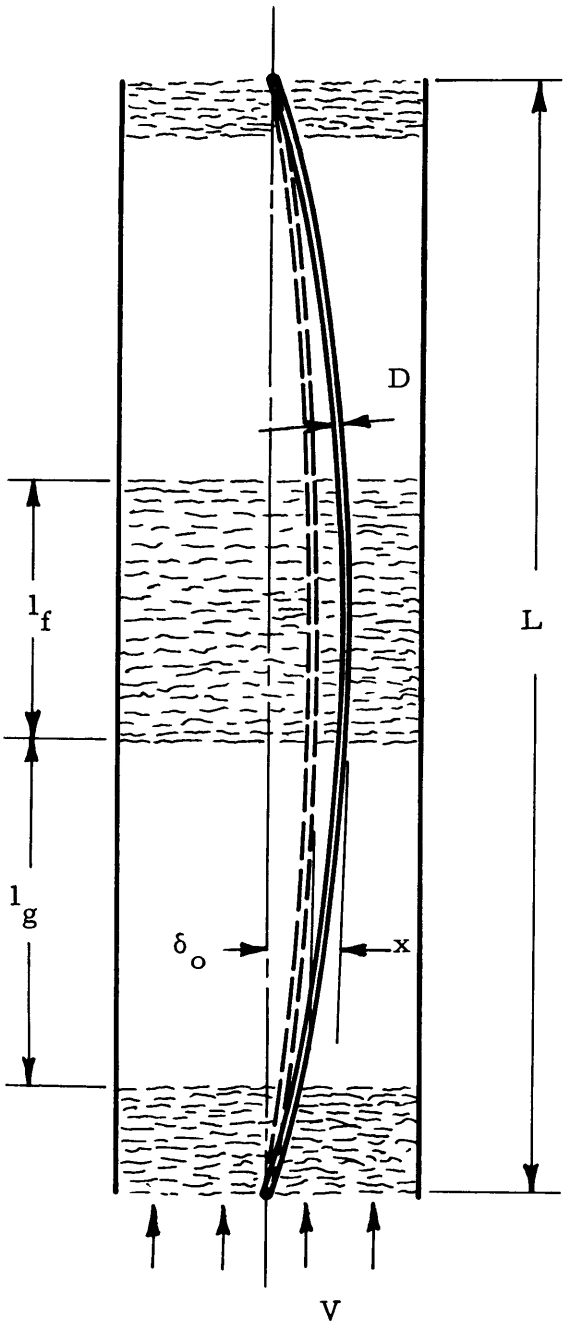

Fig. 10. Fuel Rod Model.

and the total force normal to the rod axis will be

$$F = \frac{2\delta}{L} \int_{L/2}^{L} \rho V^2 D \, dy - \frac{2\delta}{L} \int_{o}^{L/2} \rho V^2 D \, dy \qquad (10)$$

where $\delta = \delta_o + x$. Having combined with Eqs. 7 and 8, Eq. 10 becomes

$$F = \frac{D V \delta}{L\omega_k} (1-a) \rho_f V^2 \left(6-8 \cos \frac{\omega_k L}{2V} + 2 \cos \frac{\omega_k L}{V}\right) \sin (\omega_k t + \phi) \qquad (11)$$

Since in the present analysis the phase angle ϕ is of no interest it can be discarded. Then Eq. 11 can be written in the form

$$F = \frac{DV}{L\omega_k} B^{1/2} \delta P \sin \omega_k t \qquad (12)$$

where P is the mean momentum flux and is

$$P = (1-a) \rho_f V^2 \qquad (13)$$

The system geometric variables are in the term "B" which is defined as

$$B = 6-8 \cos \frac{\omega_k L}{2V} + 2 \cos \frac{\omega_k L}{V} \qquad (14)$$

The substitution of Eq. 6 into 14 yields

$$B = 6 - 8 \cos \frac{a_L}{l_g} \pi + 2 \cos \frac{a_L}{l_g} 2\pi \qquad (15)$$

It can be seen from Eqs. 14 and 15 that, B has a minimum value equal to zero when $\omega_k = 0$, i.e., in the bubbly flow or mist flow regime; it has a maximum value equal to 16 when $a_L/l_g = 1$, i.e., along the whole length of the rod there is only one bubble and one slug.

If we treat the fuel rod model as a simple system without considering the effect of damping then the equation of motion of the rod is

$$M_e \ddot{x} + k x = F \tag{16}$$

The natural frequency of the system is

$$\omega_k = \sqrt{\frac{k}{M_e}} \tag{17}$$

To simplify the analysis further the spring constant of a uniformly loaded beam with freely supported ends is adopted for k in Eqs. 16 and 17, namely

$$k = \frac{384\ EI}{5L^3} \tag{18}$$

The combination of Eqs. 12 and 16 gives the following differential equation

$$M_e \ddot{x} + (k - NP \sin \omega_k t)\ x = N \delta_o P \sin \omega_k t \tag{19}$$

where

$$N = \frac{DVB^{1/2}}{L\omega_k} \tag{20}$$

Equation 19 describes the motion of a system having variable elasticity. This implies that owing to the fluctuation of momentum flux in two-phase flow a time varying stiffness is added to the original constant stiffness of the rod. This time varying term has the same frequency of the pulsating momentum flux.

4.2 Stability

The stability of the system with variable elasticity will depend on the relative magnitudes of ω_n and ω_k as well as those of the original stiffness k of the rod and the amplitude of the time dependent stiffness NP.

Figure 11 is the diagram showing the stability of a system with variable elasticity[12]. The periodic variation of stiffness in this system is not sinusoidal but rectangular. Nevertheless, the general behavior of both systems will be much the same. Referred to Fig. 11,

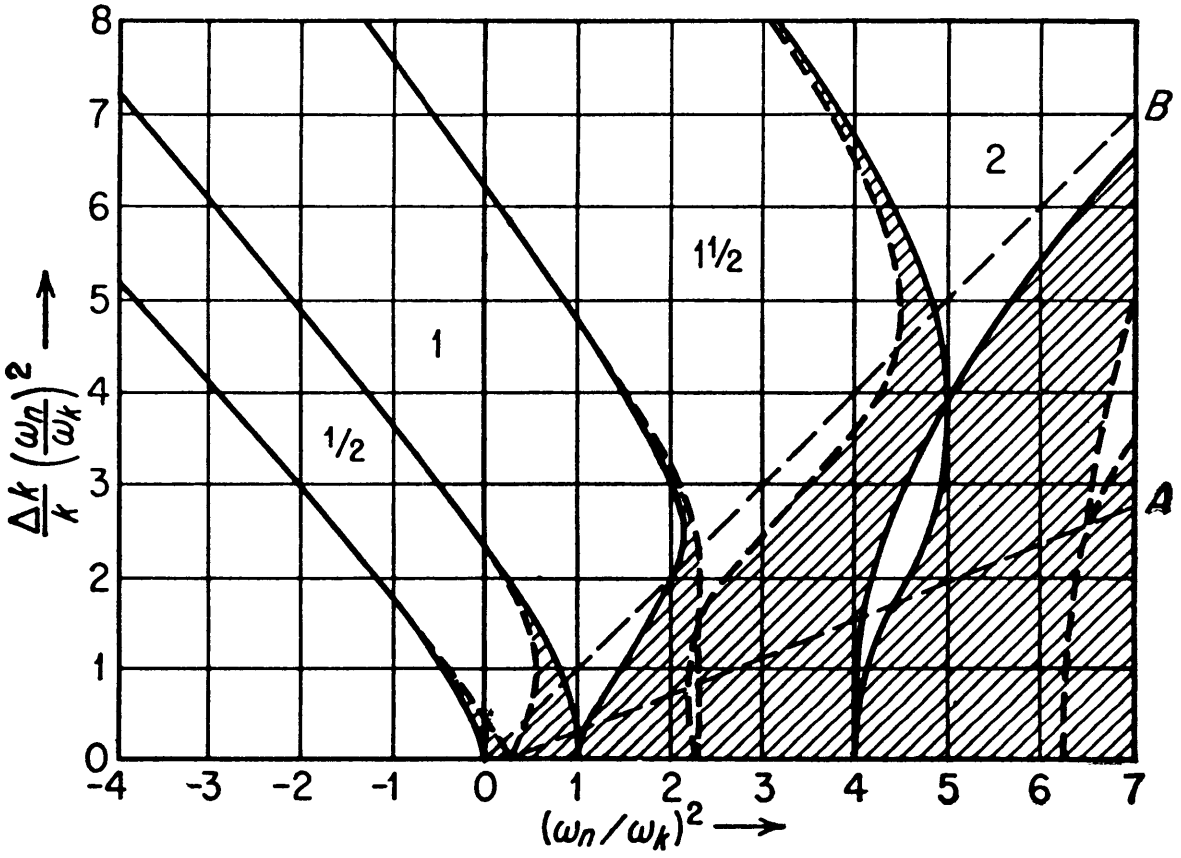

Fig. 11. Fundamental Diagram Determining the Stability of a System with Variable Elasticity. The shaded regions are stable and the blank regions are unstable.

the product NP in Eq. 19 is the term corresponding to Δk in Fig. 11. In Fig. 11, the shaded regions are stable and the blank regions are unstable. The initial deflection δ_o appears only in the forcing function term of Eq. 19. Therefore, the system will still be unstable even if there is no initial deflection of the rod so long as the ratios of ω_n/ω_k and NP/k are in the blank regions since in a two-phase flow system disturbances are inevitable. From the diagram it is obvious that, for stable operation of the system, one would like to have conditions such that $\omega_n > \omega_k$ and $k > NP$. In other words, a stiff rod and a low flow velocity are to be preferred. If the requirements of stable operation were based entirely on this diagram one would probably get an extremely low flow velocity and very high stiffness of rod. This may not be practical fuel rod design. Thus, as a stabilizing factor, the damping of such a system must be taken into consideration in any practical design. In this respect a hollow bar filled with fuel pellets is a good fuel rod structure because this will have higher damping than a solid fuel rod.

4.3 Prediction of the Vibration Amplitude of the Fuel Rod

It is a reasonably good approximation to use the average stiffness of the rod, i.e., the original stiffness k, in the calculation of this variable elasticity system provided that NP>k and the system is stable. The actual calculation procedure will depend on what kind of data is available.

Case A - If only predominant frequency of the unsteady momentum flux of flow is known then the value of P can be computed by Eq. 13. The equation of motion will have the form

$$\ddot{x} + \frac{C}{M_e}\dot{x} + \omega_n^2 x = \frac{\delta_o NP}{M_e} \sin \omega_k t \qquad (21)$$

and the maximum amplitude of the vibrating rod is

$$x_o = \frac{\frac{NP}{M_e}\delta_o}{\left(\frac{C}{M}\right)^2 \omega_k^2 + (\omega_n^2 - \omega_k^2)^2} \qquad (22)$$

Case B - When the rms value of momentum flux is available it

should be used as the value of P in Eqs. 21 and 22. This will give a more accurate result than in Case A, because the value of P obtained from Eq. 13 is a much simplified description of a real two-phase flow.

Case C - If the power density spectral curve of the momentum flux $S_p(\omega)$ is available then one can obtain the power density spectral curve of the rod deflections $S_x(\omega)$ through the following transferring process. In Eq. 21 the term P sin $\omega_k t$ should be replaced by the real history of momentum flux P(t). This gives

$$\ddot{x} + \frac{C}{M_e}\dot{x} + \omega_n^2 x = \frac{\delta_o N}{M_e} P(t) \tag{23}$$

and the transfer function is

$$H(\omega) = \frac{\frac{N}{M_e}\delta_o}{\omega_n^2 - \omega^2 + i\frac{C}{M_e}\omega} \tag{24}$$

Consequently, the power density spectrum of the excitation is

$$S_x(\omega) = \frac{(\frac{N}{M_e}\delta_o)^2}{(\omega_n^2 - \omega^2)^2 + (\frac{C}{M_e})^2\omega^2} S_p(\omega) \tag{25}$$

A process similar to either one of the three transferring methods described in Chapter 3 can be used in Eq. 25.

5. RESULTS AND DISCUSSION

5.1 Results

It can be seen from the experimental data given in Appendix C that the general criteria of the steady and unsteady components of the momentum fluxes in a two-phase flow are quite different. With the magnitude of the steady momentum flux of each test indicated by the figures in the column "Average Force" and the relative magnitude of the unsteady momentum flux represented by the "Area under PSD Curve", the comparison of the data of tests No. 3, 4, 11 and 12 shows that the greatest unsteady momentum flux can be associated with relatively low values of steady momentum flux. At conditions of large steady momentum flux the unsteady component may be very small. In this respect, the ratio of air and water flow rates, in terms of either quality or void fraction, plays an important role. For the steady momentum flux, one can expect it to increase with decreasing quality through the entire quality range from 0 per cent to 100 per cent. This trend can be visualized by comparing the data of tests No. 1, 2 and 10 or No. 5, 6 and 13. The same is not true for the unsteady momentum flux. In the preliminary experiments large pulsations of momentum flux were found in the quality range from one per cent to 6 per cent. Above 10 per cent quality no appreciable fluctuation has been detected. This agrees with Andeen's results[8] and indicates that the slug flow is probably a suitable model for the analysis of unsteady momentum fluxes. Since the mist flow pattern would be expected at high quality and bubbly flow pattern at very low quality. By physical reasoning, the unsteadiness of the momentum flux in either flow regime will be very small. The same trend was seen in Semenov's work, where the wall pressure fluctuation became very small as the value of flowing void fraction β of the air-water mixture was greater than 0.99[1]. However, the effects of average flow velocity on both the steady and unsteady momentum fluxes are similar. Both components of momentum fluxes increase with increasing velocity.

In the power spectral density curves the energy was distributed in a very broad frequency band. See Fig. 12 for example. The major part of the energy is contained in the range of 10 cycles/sec. to 30 cycles/sec. rather than any single indentifiable frequency. Beyond

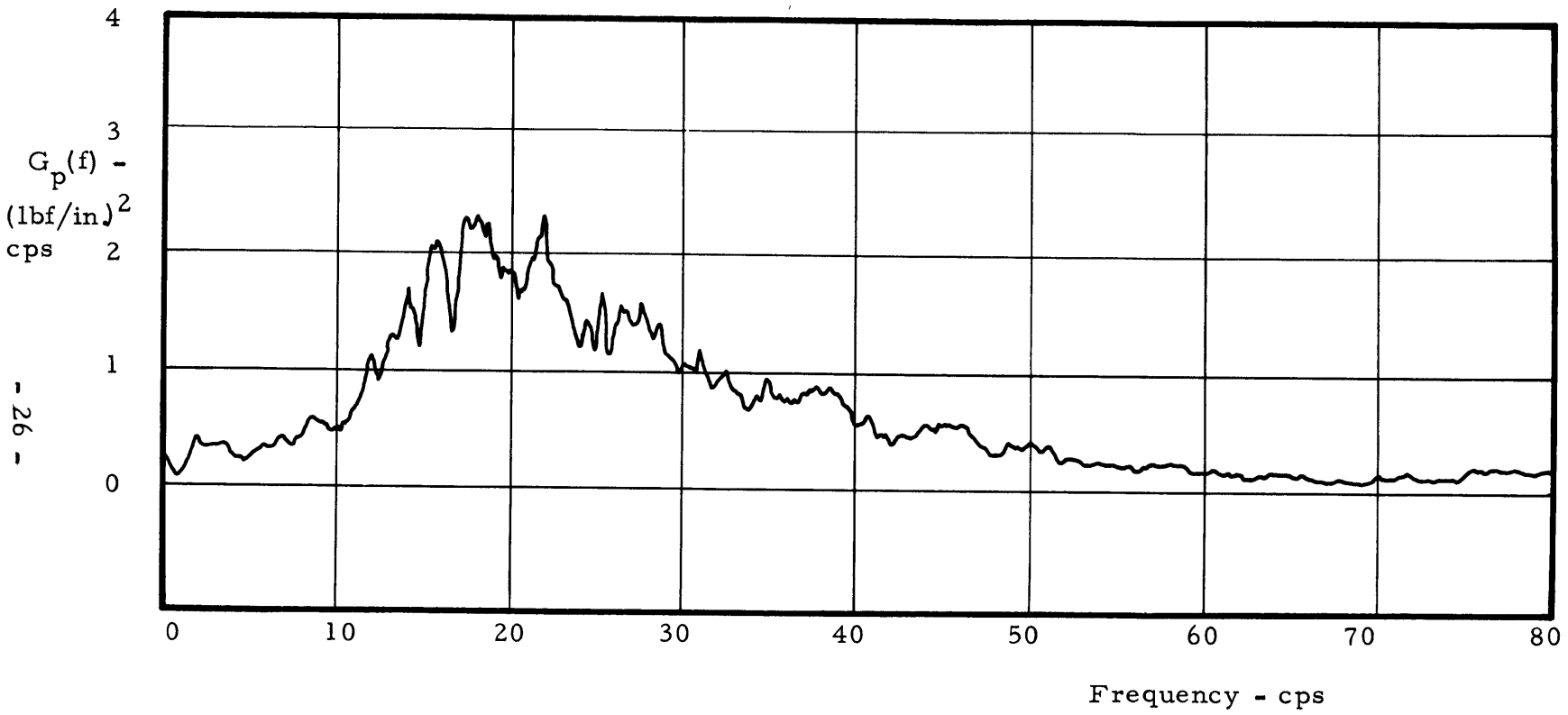

Fig. 12. Power Spectral Density of Momentum Flux of Test No. 13.

50 cps the values of $G_p(f)$, i.e., the ordinates of the spectral density curve, are very small. This indicates that the momentum flux fluctuations are insignificant in the high frequency range. The effect of high flow velocity is to shift the hill of the power spectral density curve toward the higher frequency range.

5.2 Effects on Fuel Rod

Due to the fluctuation of the momentum flux in two-phase flow the fuel rod can become a vibratory system with variable elasticity. Under certain conditions this may lead to unstable motion of the system, that is, the amplitudes become larger and larger with time. Generally speaking, high natural frequency of the fuel rod and low velocity of the two-phase flow are good for obtaining stable motion. A high damping is also desirable.

By using the power spectral density curve of the momentum flux the prediction of the amplitude of the fuel rod in two-phase flow induced vibration will give the most practical result. Because the other two methods are based on the assumption that the momentum flux fluctuates at some single frequency, they will give answers higher than the real amplitude. If the natural frequency of the rod can be kept away from the exciting frequency range, where the major part of the energy is, then the amplitude of the fuel rod vibration will be negligibly small.

5.3 Projected Program

The measuring technique and the method of data processing developed in the preliminary stage were proven to be adequate. Therefore, they will be applied in further investigations of the unsteady momentum fluxes. In particular, the combined filter system having the performance curve shown in Fig. 6 will be adopted in the signal recording circuit; the data processing is to be carried by the spectral analysis system in Fig. 7.

Emphasis will be laid upon the survey of the important variables such as the flow velocity and the ratio of gas and liquid flow rates. Because of the important engineering applications, the momentum flux pulsation in two-phase flow of a steam-water mixture with heat addition will also be examined in detail.

APPENDIX A

Calibration of Power Spectral Density Curve

Inside the pressure vessel the beam was forced to vibrate at a frequency of 5 cps by a mechanical device which was set at the middle part of the beam. Through the recording system shown in Fig. 2 this signal was recorded on both the tape and brush recorders. The signal appeared to be a sine wave. At this low frequency the static force deflection relation of the beam can still be applied with very little error. Therefore, the rms value of the force acting on the beam was calculated from the VTVM reading and was found to be F - 1.74 lbf. After the spectral analysis of this 5 cps signal, kinks were found at the starting part of the power spectral density curve. This was thought to be because of the inability of the instruments to work in the very low frequency region around 1 cps. For accurate area measurement a 20 cps sine wave was fed into the recording system from the sine wave generator shown in Fig. 2. The amplitude of the recorded signal appeared equal to that of the 5 cps signal. The spectral density curve of this sine wave is shown in Fig. 13, which has the same general shape as the 5 cps curve-except there is no kink. The area under the $G_F(f)$ curve was measured to be A_{20} = 2.14 in.^{2}. Then the area scale was computed as F^2/A_{20} = 1.42 lbf^2/in.^{2}. As the experimental result of test No. 13 was used for illustration, the area under the $G_p(f)$ curve in Fig. 12 was found to be $A_{\#13}$ = 3.3 in.^{2}. In order to get the rms value of the momentum flux per unit area of flow, the area scale of Fig. 12 would be $C_A = F^2/A_{20}(A_{pipe})^2$ = 14.8 (lbf/in.^{2})^2 per inch of the area under the curve and the ordinate scale is C_{Gp} = 14.8/10 = 14.8 (lbf/in.^{2})^2/cps per inch of height in the diagram. From Eq. 3 we have $E(p^2) = C_A \cdot A_{\#13}$(lbf/in.^{2})^2, and $P_{rms} = \sqrt{E(p^2)} = \sqrt{C_A \cdot A_{\#13}}$ = 7(lbf/in.^{2}).

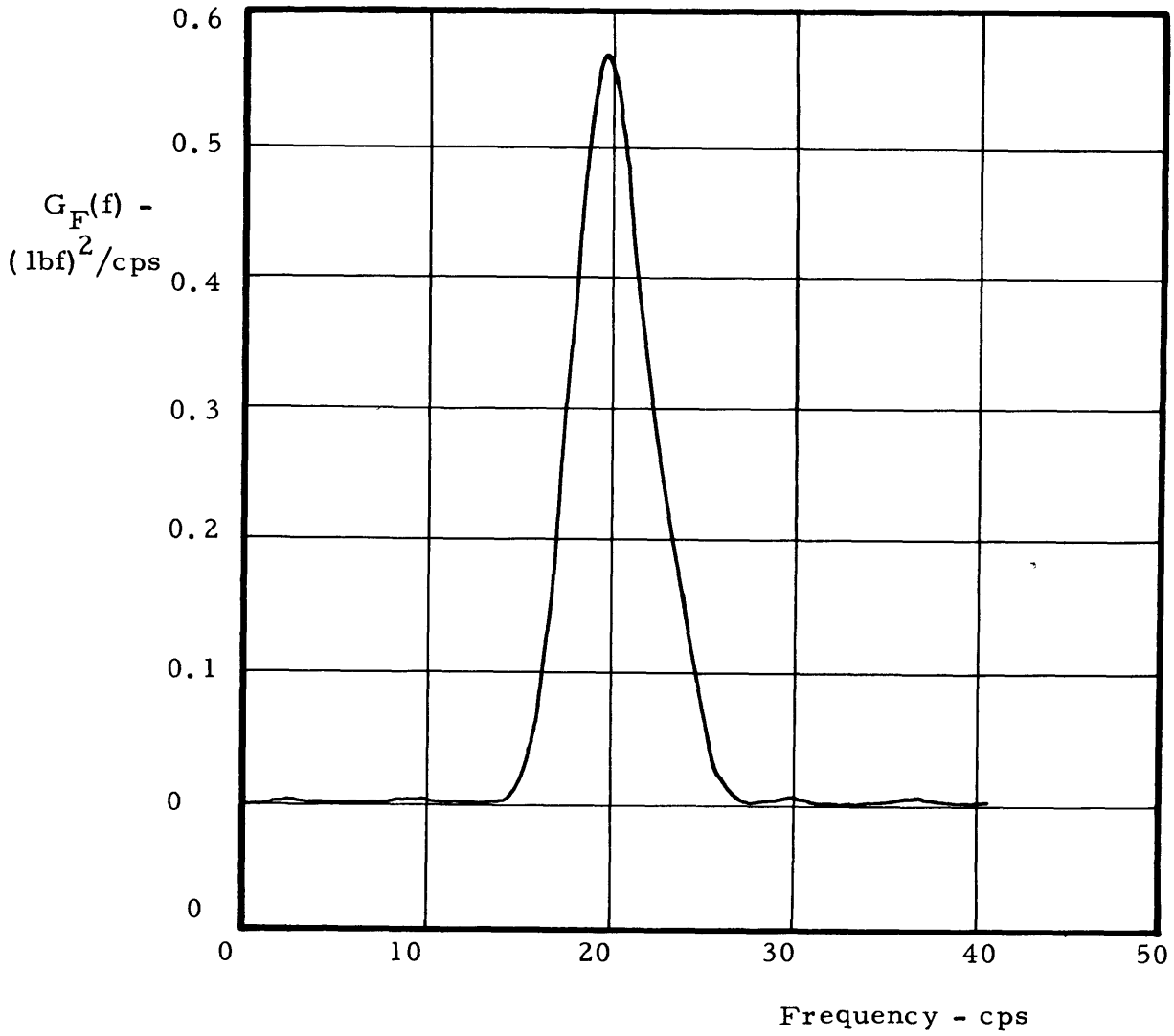

Fig. 13. Power Spectral Density of 20 cps Sine Wave.

APPENDIX B

Transfer Function

The beam and turning tee combination is considered to be a simple linear time-invariant vibratory system. When a force F is applied to the system its equation of motion is

$$M_e \ddot{x} + c\dot{x} + kx = F \tag{26}$$

The beam system is excited by the momentum flux of the two-phase flow, i.e., a force; the quantity picked by the LVDT is the displacement of the beam. Therefore, the excitation history to the system is F(t) and the response history is x(t). To find the transfer function $H(\omega)$ of the system in the frequency domain it is assumed that

$$\begin{aligned} F(t) &= e^{i\omega t} \\ x(t) &= H(\omega)\, e^{i\omega t} \end{aligned} \tag{27}$$

By substituting Eq. (27) in Eq. (26), canceling $e^{i\omega t}$, the solution $H(\omega)$ is then obtained as

$$H(\omega) = \frac{1}{k - M_e\omega^2 + ic\,\omega} \tag{28}$$

The equivalent mass M_e is the sum of the mass of the turning tee and one-half of the mass of the beam. It was obtained by weighing the beam and the turning tee, separately. The stiffness k was measured through the static load test of the beam. For the determination of the damping coefficient c the logrithmic decay rate $e^{(\pi c/2M_e\omega_m)}$ was measured from the pluck test picture then the value of c was computed. It was found that M_e = 0.98 lbm, k = lbf/in and c = 2.65×10^{-3} (lbf-sec/in). As a function of frequency the reciprocal of the transfer function is

$$\frac{1}{H(\omega)} = (505000 - 142.8\, f^2 + 0.0101\, f^4)^{1/2} \tag{29}$$

where f is the frequency in cycles per second. Equation (29) was plotted in Fig. 6.

APPENDIX C

Experimental Data

Test No.	Air Flow Rate lbm/hr.	Water Flow Rate lbm/hr.	Quality Per Cent	Average Velocity ft/sec.	Average Force lbf	Area under PSD Curve[+]
1	25.7	2500	1.0	49	0.6	17
2	49.6	2500	1.9	90	1.1	20
3	72.5	2500	2.8	129	1.3	41
4	92.5	2500	3.7	164	2.2	46
5	130.0	2500	4.9	228	2.9	27
6	130.0	2070	5.9	228	2.3	32
7	195.0	2500	7.3	339	4.5	25
8	186.0	1950	8.7	324	3.7	13
9	240.0	2500	8.8	417	5.3	29
10	81.5	695	10.5	150	0.5	
11	338.0	1660	17.0	618	7.1	
12	364.0	1290	22.0	625	7.0	
13	115.0	2880	3.8	200	3.0	

+ Figures in this column are the relative magnitudes of the areas under the Power Spectral Density curves. The fluctuations of momentum flux in tests No. 10, 11 and 12 are so small that their spectral density curves are almost straight lines. A different scale was used in the spectral analysis of test No. 13, so the figure is not given here.

APPENDIX D

Numerical Example for Predicting the Vibration Amplitude of the Fuel Rod

In this example the data of test No. 13 were used. The physical quantities regarding the fuel rod and others needed in the calculation were assumed. A reasonable damping coefficient was also introduced. These data are:

$\rho_f = 62.4$ lbm/ft^3 $\quad a = 0.97$ $\quad \omega_k \tilde{=} 16 \times 2\pi$ rad/sec

$L = 56$ inches $\quad D = 0.5$ inches $\quad D = 30 \times 10^6$ lbf/in.^{2}

$\rho_r = 0.28$ lbm/in.^{3} $\quad \delta_o = 0.125$ inches $\quad c = 0.01$ lbf/sec/in.

$B = 4$

Case A - Substituting the given data into Eqs. 13, 17, 18 and 20

$P = 16$ lbf/in.^{2}, $\quad k = 40$ lbf/in., $\quad N = 7/16$ in., $\quad NP = 7$ lbf/in.,

and $\omega_n = 100$ rad/sec. $= \omega_k$.

From Eq. 22 the amplitude was calculated to be $x_o = 0.8$ inch.

Case B - From Appendix A by measuring the area under the $G_p(f)$ curve of test No. 13 in Fig. 13 the rms value of the unsteady momentum flux is $P_{rms} = 7$ lbf/in^2.
From Eq. (22) $x_o = 0.35$ inches.

Case C - By substituting the given data into Eq. 25 it became

$$G_x(f) = \frac{189}{(10,000 - 39.5\, f^2)^2 + 249\, f^2}\, G_p(f) \qquad (30)$$

With the help of the $G_p(f)$ curve in Fig. 12, Eq. 30 was plotted in Fig. 14. The peak of this curve is $G_x(16) = 5 \times 10^{-3}$ in.^{2}/cps which was not shown in the diagram. Similar to Eq. 3 the mean square of the vibration amplitude is

$$E(x)^2 = \int_o^\infty G_x(f)df \qquad (31)$$

Approximately, $E(x^2) = 1/2\,(14.4)(5 \times 10^{-3}) = 0.036$ in.^{2} and $x_{rms} = 0.19$ in.

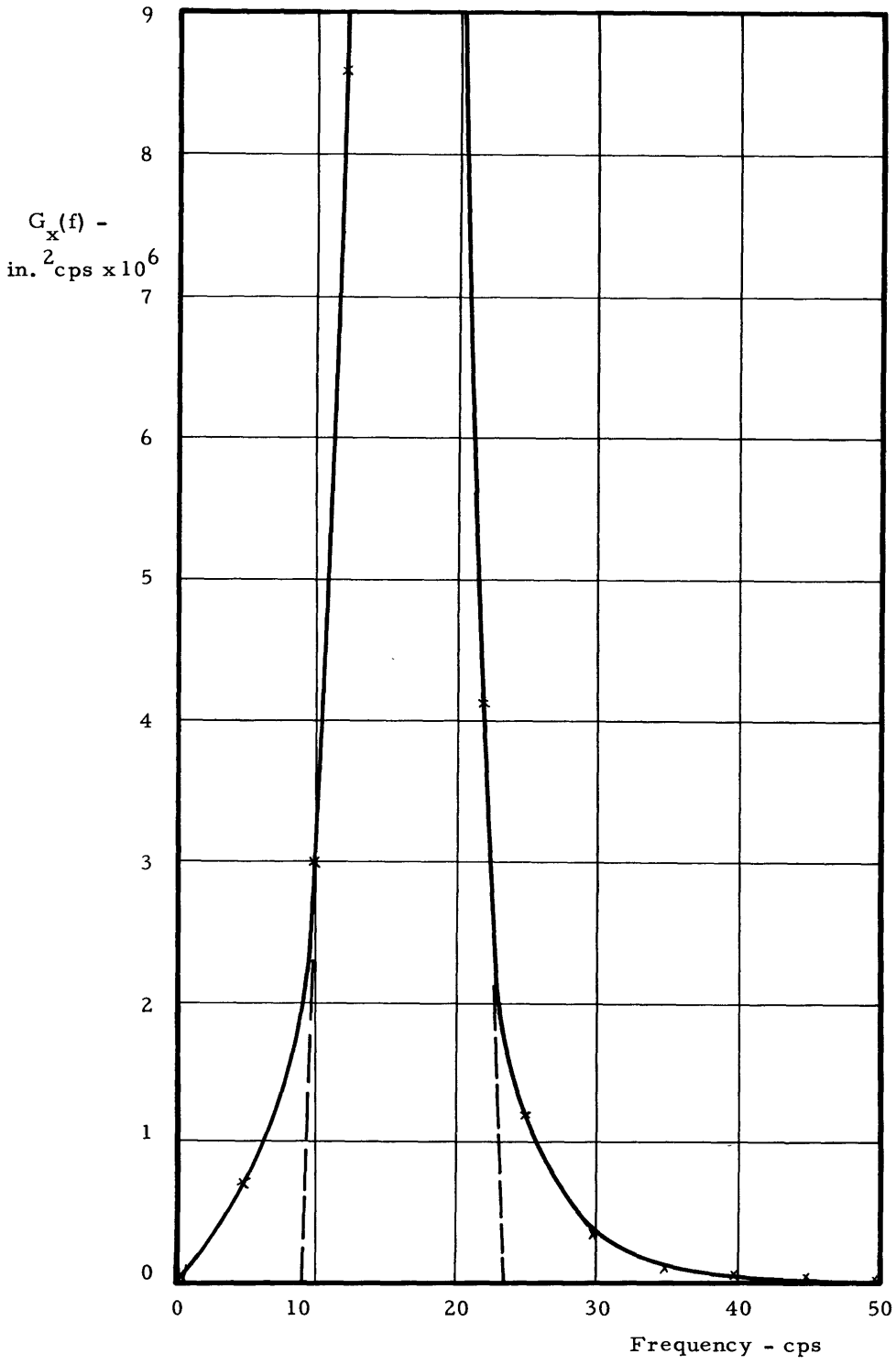

Fig. 14. Power Spectral Density of Fuel Rod Amplifier (computed).

REFERENCES

1. Semenov, N.I., "Pressure Pulsations During the Flow of Gas-Liquid Mixtures in Pipes," Heat Power Engineering Part I, USAEC, Division of Technical Information, AEC-tr-4496, December 1961, translated.

2. Hubbard, M.G., and Dukler, A.E., "The Characterization of Flow Regimes for Horizontal Two-Phase Flow," Proceedings of the 1966 Heat Transfer and Fluid Mechanics Institute.

3. Rosenberg, G.S., and Youngdahl, C.K., "A Simplified Dynamic Model for the Vibration Frequencies and Critical Coolant Flow Velocities for Reactor Parallel Plate Fuel Assemblies, "Nuclear Science and Engineering, 13, 1962, pp. 91-102.

4. Wambsganss, M.W., Jr., "Second Order Effects as Related to Critical Coolant Flow Velocities and Reactor Parallel Plate Fuel Assemblies," ANL-7261, Engineering and Equipment (TID-4500) AEC Research and Development Report, November 1966.

5. Paidoussis, M.P., "The Amplitude of Fluid-Induced Vibration of Cylinders in Axial Flow," AECL-2225, Chalk River, Ontario, Canada, March 1965.

6. Burgreen, D., Byrnes, J.J., and Benforado, D.M., "Vibration of Rods Induced by Water In Parallel Flow," Trans. ASME, 992-1003, July 1958.

7. Pavlica, R.T., and Marshall, R.C., "Vibration of Fuel Assemblies in Parallel Flow," Trans. Amer. Nucl. Soc., Vol. 8, No. 2, November 1965

8. Andeen, G.B., and Griffith, P., "The Momentum Flux in Two-Phase Flow," Technical Report No. 4547-38, U.S.AEC Contract No. AT(30-1)-3301, October 1965.

9. Bendat, J.S., Piersol, A.G., Measurement and Analysis of Random Data, Wiley, New York, 1966.

REFERENCES (Continued)

10. Crandall, S.H., and Mark, W.D., Random Vibration in Mechanical Systems, Academic Press, New York, 1963.

11. Gurski, R.J., Static and Dynamic Modeling of a Pressure Controlled Subsonic Fluid Jet Model. Thesis (ScD.), Mass. Inst. of Tech., Dept. of Mech. Engr., 1965.

12. Den Hartog, J.P., Mechanical Vibration, McGraw-Hill, New York, 1965.